CONFERENCE PRE-PRINT

ANALYTICAL APPROACH TO CALCULATION OF DISRUPTION-INDUCED VERTICAL FORCE ON THE TOKAMAK WALL

V.D. PUSTOVITOV
National Research Centre "Kurchatov Institute"
Moscow, Russian Federation
Email: Pustovitov_VD@nrcki.ru

Abstract

Integral vertical disruption force acting on the tokamak vacuum vessel wall is analytically calculated starting from the Maxwell equations and the Ohm's law for the wall. With axial symmetry, these allow transformations of the integral to the expression explicitly showing the key parameters in the task. It is confirmed, in particular, that the toroidal current density in the plasma fully determines the plasma contribution into the force, while the knowledge of the poloidal halo current is not needed. Another finding is that, for the wall current description, two modes with different decay rates are required. The force is examined with emphasis on the post-disruption stage. The model proposed in (Miyamoto 2011 *Plasma Phys. Control. Fusion* **53** 082001) is revised. The study is fully analytical.

1. INTRODUCTION

For the ITER discharges with 15 MA current, the disruption-induced vertical force F_z^w on the vacuum vessel (VV) wall is expected on the level of 100 MN (though with some scatter in the predictions: about 120 MN in [1] or 75 MN in [2]). Such marginally tolerable loads can pose severe operational limitations. This and the absence of sufficient knowledge make the reduction of the vertical force in large tokamaks an important topic [3].

Despite a long history of research, there are still unresolved questions and even conflicts between theoretical concepts. One was inspired by a formula for F_z^w proposed in [4] and recently criticized in [5]. Another one is related to the role of the halo currents. The wide-spread opinion is that "the forces associated with halo currents are a major contributor to the vertical force acting on the torus vessel during a disruption" [6]. However, in a stark contrast, it was stated that the total vertical force is largely unaffected when the amount of halo current changes [2]. Being solidly supported by reliable 2D calculations and analytical arguments for the forces due to wall halo currents and toroidal currents in the open field line region, this deserves a closer inspection.

A reliable basis is needed for discussion of these and related issues. To cover the existing approaches, it has to be built from the first principles with minimal assumptions. These are usually introduced to overcome the uncertainties in the plasma description, though actually could be postponed till clarification of the necessary set of relevant parameters. The meaning of this can be illustrated by the question: do we really need a detailed description of the halo current in the task? A positive answer would seem natural, but premature before integration of $\mathbf{j}\times\mathbf{B}$ over the wall (here, the current density and magnetic field, respectively). And finally the opposite will be shown.

The derivations here start from the Maxwell equations. Initially only axial symmetry is assumed. There are no simple or generally accepted rules for description of the halo current density $\mathbf{j}_h$ in tokamaks, but two properties allow to transform the expression for F_z^w without the knowledge of the poloidal component of $\mathbf{j}_h$: the axial symmetry and the closure of the lines of $\mathbf{j}_h$ inside the full system plasma + wall ($w+ = pl + w$). The expression is further simplified by accounting for the fact that the toroidal currents do not produce an integral force on themselves. After these transformations, the general result (justified in Sec. 2)

$$F_z^w + F_z^{pl} = -\int_{w+} j_\zeta B_r^c dV \qquad (1)$$

is already meaningful. In particular, it allows evaluation of the findings in [2] and constructions in [4]. Here j_ζ is the toroidal current density, and B_r^c is the radial component of the external magnetic field produced by the poloidal coils. The presence of only j_ζ in (1) is consistent with a numerical proof in [2]. The integration over

the volume includes both the plasma and wall. The latter is unavoidable, which refutes the statement in [4] that it is possible to calculate the vertical force F_z^w without explicitly using the knowledge of the eddy current in the vessel.

The latter is obviously incorrect when only the integral over the wall remains in (1), as it occurs after the end of disruption, when $\mathbf{j}^{pl} = 0$. This unexplored area attracts attention because some computations show [7–11] that the post-disruption force F_z^w can be large enough.

Here, the force generation is treated as a two-stage process, during the disruption itself and resulting due to the wall current evolution after the disruption. This combines two dynamic tasks: one with the plasma-wall electromagnetic interaction producing a large current in the toroidal VV wall, and another with redistribution and decay of the currents induced in the wall. The second step is needed because a rapid CQ cannot produce a sizable integral force [12], but the force must appear afterwards.

Description of the wall as a resistive conductor becomes a part of the task. In the model recommended for ITER and future tokamaks in [4], it was proposed to treat the vessel current decay "uniformly in space", which means with a single time constant. This would give a pure exponential decay of the post-disruption force F_z^w, while the CarMa0NL computations [7] demonstrated essentially different behaviour with a phase of F_z^w growing to quite a high level. This conflict of the predictions is also analysed.

2. GENERAL EXPRESSION FOR THE VERTICAL FORCE ON THE WALL

By definition, the net electromagnetic vertical force on the wall is

$$F_z^w = \mathbf{e}_z \cdot \int_w \mathbf{j} \times \mathbf{B} dV \,, \tag{2}$$

where $\mathbf{e}_z = \nabla z$ is the unit vector along the main vertical axis of the torus, the integration is performed over the wall volume. A similar force $\mathbf{e}_z \cdot \mathbf{F}^{pl}$ on the plasma is given by the same expression with integration over the plasma. For the description of axisymmetric events, we can use the representation

$$\mathbf{j} \times \mathbf{B} = \mathbf{j}_p \times \mathbf{B}_t + \mathbf{j}_t \times \mathbf{B}_p \tag{3}$$

with subscripts *p* and *t* denoting the poloidal and toroidal components, respectively. In such a model, $\mathbf{j}_p \times \mathbf{B}_p$ is, at least, negligible or even zero, $\mu_0 \mathbf{j}_p = \nabla(rB_t) \times \nabla\zeta$ and $2r^2 \mu_0 \mathbf{j}_p \times \mathbf{B}_t = -\nabla(rB_t)^2$. Therefore, $2\mu_0 \mathbf{e}_z \cdot (\mathbf{j}_p \times \mathbf{B}_t) = -\nabla \cdot (B_t^2 \mathbf{e}_z)$ because $\nabla \cdot [f(r)\mathbf{e}_z] = 0$ (with $f = 1/r^2$ in this particular case). By using this property again we obtain

$$\mathbf{e}_z \cdot \int_{w+} \mathbf{j}_p \times \mathbf{B}_t dV = 0 \tag{4}$$

with integration performed over the toroidal volume bounded by the axially symmetric surface $w+$ on the outer side of the wall, where $rB_t = \text{const}$. These transformation lead to

$$F_z^w + F_z^{pl} = \mathbf{e}_z \cdot \int_{w+} \mathbf{j} \times \mathbf{B} dV = \mathbf{e}_z \cdot \int_{w+} \mathbf{j}_t \times \mathbf{B}_p dV \,. \tag{5}$$

Since F_z^{pl} must be several orders smaller than F_z^w [12], this can be used as a starting expression for the vertical force on the wall. The notation refers to the conventional cylindrical coordinates (r, ζ, z) related to the main vertical axis of the torus.

The result in (5) is determined by the toroidal component of $\mathbf{j}$, while $\mathbf{j}_p$ is absent there. The plasma-wall separation or contact have not been constrained on the way to (5) that must be valid with or without halo current $\mathbf{j}_h$ traditionally introduced as the poloidal current flowing from the plasma into the wall and back. The halo current disappeared in (5) after the integration over the volume inside $w+$, where the lines of $\mathbf{j}_h$ are fully closed. Without trace of $\mathbf{j}_h$ in (5), the dependence of the force on $\mathbf{j}_h$ must be implicit through $\mathbf{j}_t$.

Equation (5) contains the full magnetic field

$$\mathbf{B} = \mathbf{B}^{pl} + \mathbf{B}^{c} + \mathbf{B}^{w} \tag{6}$$

automatically accounting for electromagnetic interaction of all current-carrying elements. Here *pl*, *c* and *w* denote, respectively, plasma, external coils and vacuum vessel wall. Since the integral force self-produced by the system *pl* + *w* must be zero, only $\mathbf{B}_p^c$ will remain in (5). It is then reduced to equation (1), which is a purely electromagnetic relation for an axisymmetric system separated from the external currents by the toroidal surface $w+$ ($\mathbf{j} = 0$ on $w+$). Being obtained without assumptions on the plasma properties, it is compatible with any plasma model. The important point is that the tokamak plasma is a lightweight medium, and its motion toward the wall is slow enough for disregarding the force on the plasma F_z^{pl} in (1).

3. REDUCTION OF (1)

In a tokamak, the external poloidal magnetic field can be represented as

$$\mathbf{B}_p^c = \mathbf{B}_\perp^c + \mathbf{B}_q^c + \ldots, \tag{7}$$

where $\mathbf{B}_\perp^c$ is the uniform vertical component, and $\mathbf{B}_q^c$ is the quadrupole one. The standard analytical theory of plasma equilibrium was developed for a tokamak with a circular plasma and $\mathbf{B}_\perp^c \neq 0$ only. This field is needed for plasma positioning. Incorporation of $\mathbf{B}_q^c$ is a step ahead allowing for the control of plasma elongation, see [13] and references therein. These two fields must be the dominant harmonics, while those with higher polarities (unaccounted for in (7)) can be either "by-products" appearing because of the discrete structure of the external currents in real tokamaks, or intentionally created for additional shaping of the plasma.

One can see that $\mathbf{B}_\perp^c$ drops out of (1), which means that the vertical force F_z^w must be zero in a tokamak with such a field only (with $\mathbf{B}_p^c = \mathbf{B}_\perp^c$). It is interesting that the presented equations lead to this general conclusion irrespective of the plasma parameters, scenarios of the discharge or the plasma/wall shapes. This makes $\mathbf{B}_q^c$ the main term in (7) necessary for calculating F_z^w.

Equation (1) can be rewritten as

$$F_z^w + F_z^{pl} = \int\limits_{w+} j_\zeta \frac{\partial \psi^c}{\partial z} dS_\perp , \tag{8}$$

where we have used the identity $dV = 2\pi r dS_\perp$ and relation $2\pi \mathbf{B}_p^c = \nabla\psi^c \times \nabla\zeta$ with ψ^c being the poloidal flux created by the currents in the control coils external to the torus $w+$. Therefore $\mathrm{div}(\nabla\psi^c / r^2) = 0$ within the volume $w+$. In the large-aspect-ratio, we can use the multipole expansion [13]

$$\psi^c = \psi_0^c + \pi r^2 B_\perp^c + \psi_q^c + \ldots \tag{9}$$

corresponding to (7). Here ψ_0^c is the time-depending constant describing the flux consumption for generating the toroidal electric field. The second term appears because of the uniform vertical field $B_\perp^c$ produced for controlling the plasma horizontal position, and

$$\psi_q^c = C_q[(z - z_q)^2 - (r - R_q)^2] \tag{10}$$

(being a solution in the limit $r / R_q \to 1$) is responsible for the plasma elongation. The presence of z_q and R_q in (10) allows for the shift of the null point of $\mathbf{B}_q^c$ with respect to the VV centre. For the relation of C_q to the plasma parameters, see [13], where the external task for an "elongated" tokamak plasma was analytically solved with account of the toroidal corrections in the linear approximation.

With the last two relations, substitution of ψ^c into (8) yields

$$F_z^w + F_z^{pl} = 2C_q(M_{IZ}^{pl} + M_{IZ}^{w}), \tag{11}$$

where

$$M_{IZ}^{\alpha} \equiv \int\limits_{\alpha} j_\zeta (z - z_q) \frac{r^2}{R_w^2} dS_\perp , \tag{12}$$

and α is either *pl* or *w*. This is the most convenient form for comparisons with various expressions relating F_z^w to so-called vertical current moment, see Eq. (2) in [3] and an equation in section 4.2.2 in [11].

In [3], the force reduction during mitigated disruptions was attributed to the reduction of M_{IZ}^{pl}, defined there like (12) with r^2/R_w^2 replaced by unity. More important is the absence of z_q in [3], especially in view of the fact that z_q is also present in M_{IZ}^w. The latter quantity did not appear in [3, 11], the integration in (12) was performed over the plasma only. It is explained in [3] that this must be the full plasma region (including the SOL), but nothing is said on the currents in the wall. In our equation (11), the integration covers the wall too.

In [14], it is explicitly stated (with reference to [3]) that the vertical force on the wall is proportional to the change in the vertical current moment, which means to ΔM_{IZ}^{pl} in our notation. This could be true if $\left|\Delta M_{IZ}^{pl}\right| >> \left|\Delta M_{IZ}^{w}\right|$. However, we can immediately refer to theoretical prediction [12] that $F_z^w = 0$ in the ideal-wall limit. Then formula (11) requires that $M_{IZ}^{pl} + M_{IZ}^{w} = 0$. In this example, both "current moments" must vary synchronously in antiphase making F_z^w insensitive to M_{IZ}^{pl} so that F_z^w remains fixed irrespective of M_{IZ}^{pl} evolution. Before a final conclusion on the efficiency of the reduction strategy proposed in [3, 14], the conditions for disregard of M_{IZ}^w have to be specified and justified.

In [3], the vertical force on the wall was symbolically presented as

$$F_z^w = F_{p,c} + F_{v,c}\,, \tag{13}$$

which is the starting Eq. (1) there. With proper definitions this could be equivalent to our equations (1) and its reduced consequence (11). However, no expression for the force $F_{v,c}$ produced by the poloidal field coils on the vacuum vessel has been given in [3], and the role of $F_{v,c}$ in (13) or M_{IZ}^w in (11) has not been evaluated (the same in [14]).

We already explained that the both terms in (11) and (13) must be strongly coupled during rapid events with $\Delta M_{IZ}^{pl} = -\Delta M_{IZ}^{w}$ in the ideal-wall limit. The practical consequence is that the amplitudes of these increments must be comparable near this asymptote. Being a useful reference case in theory, this can cover only a part of the observed phenomena. In a general case we have to treat the wall as resistive. Then the balance between M_{IZ}^{pl} and M_{IZ}^w will be different, but not necessarily with dominance of M_{IZ}^{pl}.

On the contrary, it is clear that the wall terms in (11) and (13) will exceed the plasma contribution near and especially after the end of the discharge because $M_{IZ}^{pl} \to 0$ when $j_\zeta \to 0$ in the plasma. Therefore, without M_{IZ}^w in (11) or without $F_{v,c}$ in (13), the result will be precisely $F_z^w = 0$ when finally $\mathbf{j}^{pl} = 0$. This outcome of the simplified treatment with $F_z^w = F_{p,c}$ (accepted in [14] after [3]) is incorrect. Similar inconsistency can be also seen in the model [4], in addition to its other elements fairly criticized in [5]. The examples with large F_z^w developing after the end of full CQ (when $F_{p,c} = 0$) have been presented in [7] and later in [8–11].

To get a deeper insight, let us introduce $\xi_z(t)$ (coinciding with Z_{curr} defined by Eq. (4) in [3]) by the equality

$$\int_{pl} (z - \xi_z)\, j_\zeta dS_\perp = 0\,, \tag{14}$$

where $dS_\perp$ is the surface element in the perpendicular cross-section. Correspondingly, the "current centroid" ξ_z represents the geometric centre of the full plasma current, including the halo region. Then we have

$$\int_{pl} (z - z_q)\, j_\zeta dS_\perp = J(\xi_z - z_q) \tag{15}$$

irrespective of the plasma shape. The integration includes the halo area, which makes this relation universally applicable. The halo-current contributions into F_z^w is automatically accounted for in this approach. With

definition (14), the first term $J\xi_z$ in (15) is equivalent to M_{IZ} given by Eq. (4) in [3] and called there vertical current moment. The other integral in (11) can be expressed similarly to (15) by using

$$\int_w (z - z_q)\, j_\zeta dS_\perp = J_s^w b_w - J_w z_q\,, \tag{16}$$

where J_w is the net toroidal current in the wall, and $J_s^w b_w$ represents the contribution from zj_ζ.

With (15) and (16), equations (11) and (12), where we replace r^2/R_w^2 by unity (omit toroidal corrections), yield

$$F_z^w + F_z^{pl} = 2C_q[J(\xi_z - z_q) - J_w z_q + J_s^w b_w]. \tag{17}$$

This is a purely electromagnetic relation. We derived it without constraints on the plasma dynamics, plasma and wall shapes. The assumptions made on the way to (17) are minimal: large aspect ratio in (15) and (16), and the replacement of B_r^c in (1) by the quadrupole field described by (10). That is why the external field magnitude is characterized by a single constant $C_q(t)$ in (17). From the plasma, we need $J(\xi_z - z_q)$ with ξ_z defined by (14). The wall is presented by two terms in (17).

4. THE EDDY CURRENT CONTRIBUTION IN (17)

One of the main statements in [4] is that "Knowledge of eddy and halo currents is not necessarily required for estimating the net vertical force." Our equation (17) shows the opposite, and this contradiction is further discussed.

In [4], the "calculation is carried out without reference to currents in the vessel." This became possible by two reasons. First, the unexplained constraint has been used that "the vessel shields any changes of the fields in the vessel". Second, the uniform decay of the vessel eddy current was assumed in [4]:

$$j_\zeta^w(\mathbf{r},t) = j_\zeta^w(\mathbf{r},t')\exp[(t-t')/\tau_{L/R}]U(t-t') \tag{18}$$

with unit step function U and a single resistive time constant $\tau_{L/R}$.

In [5], the former assumption was called ideal and inapplicable to the ASDEX Upgrade. This was discussed as a possible reason why the final formula for F_z^w proposed in [4] could not be used for practical purposes. The analysis started in [5] is important because the model developed in [4] was proposed as "applicable to ITER and future tokamaks", see the title of that paper. The arguments advanced in [5] are reasonable, here we extend the analysis by showing that Eq. (18) must be another wrong element in [4].

Here, on the contrary to (18), we treat J_w and J_s^w in (17) as functions decaying with different rates, as it should be [8, 10, 15, 16]. The outcome will show the necessity and importance of this step greatly affecting the result compared to the case with (18). The time constants and the amplitudes of the evolving functions J_w and J_s^w must be found from equation

$$\mu_0\sigma\partial\mathbf{B}/\partial t = \nabla^2\mathbf{B}^w \tag{19}$$

in the wall. This contains full $\mathbf{B} = \mathbf{B}^{pl} + \mathbf{B}^c + \mathbf{B}^w$ on the left, and the uniform conductivity σ is assumed here.

In the mentioned model [4], relation (18) is proposed for a pure decay of j_ζ^w. A correct description of such a decay must be found by solving Eq. (19) with $\partial(\mathbf{B}^{pl} + \mathbf{B}^c)/\partial t = 0$. The latter is satisfied after the end of disruption if, in addition, $\partial\mathbf{B}^c/\partial t = 0$. Then equation (19) gives a solution for $\mathbf{B}^w$ that, for a "circular" wall, can be represented by the current density

$$j_\zeta^w = j_0^w + j_s^w \sin u\,, \tag{20}$$

where u is the conventional poloidal angle, with j_0^w and j_s^w having, respectively, different times τ_0 and τ_1 of exponential decay. For large-aspect-ratio "circular" wall these are given by [15]

$$\tau_0 = \tau_w\left(\ln\frac{8R_w}{b_w} - 2\right) \tag{21}$$

and

$$\tau_1 = \tau_w / 2, \tag{22}$$

where $\tau_w \equiv \mu_0 \sigma b_w d_w$ with b_w the minor radius, and d_w the thickness of the wall. We attract attention to the fact that $\tau_0 \neq \tau_1$ because of its principal importance in evaluation of the post-disruption force.

Indeed, substitution of $J = 0$, $J_w = J_w^0 e^{-t/\tau_0}$ and $J_s^w = J_s^w(0) e^{-t/\tau_1}$ turns equation (17) into

$$F_z^w = C_w e^{-t/\tau_0} + C_s e^{-t/\tau_1} = C_w f_w(t) \tag{23}$$

with $C_w \equiv -2C_q J_w^0 z_q$ and the time dependence described by the function

$$f_w(T) \equiv F_z^w / C_w = e^{-T} - \alpha e^{-\eta T}. \tag{24}$$

Here $J_s^w \equiv \pi b_w d_w j_s^w$, which is obtained substituting (20), $z = b_w \sin u$ and $dS_\perp = d_w b_w du$ in (16), $T \equiv t/\tau_0$,

$$\alpha \equiv \frac{J_s^w(0)}{J_w^0} \frac{b_w}{z_q}, \tag{25}$$

$$\eta \equiv \tau_0 / \tau_1 > 1. \tag{26}$$

Equations (23) and (24) show that the time evolution of the post-disruption force is determined by two dimensionless quantities α and η, and two more constants C_w and τ_0 are needed to prescribe the absolute value of F_z^w and the true time scale. Both α and C_w depend on the discharge history, while η and τ_0 are fixed machine parameters. The latter pair can be found either numerically by calculating the wall response to external magnetic perturbations or experimentally from magnetic measurements. First, we discuss the role of η.

5. REALISTIC $\eta > 1$ VERSUS $\eta = 1$ IN [4]

According to (21) and (22), for a circular wall, η depends on the wall aspect ratio only and varies between 1.55 and 2.93 for $2 \le R_w / b_w \le 4$. In [8], $\tau_0 / \tau_1 = 1.85$ was found for the VV in the COMPASS-U tokamak. Similar quantity $\tau_0 / \tau_1 = 536/295 = 1.82$ was obtained for ITER in [16].

The fact that $\eta > 1$ has important implications. With $\eta > 1$, as it must be in conventional tokamaks, and with $\eta = 1$ (equation (18) representing the model in [4]) the time evolution of F_z^w prescribed by (23) is essentially different. The best illustration of that is the consequence of (23) in the ideal-wall limit applicable during the preceding CQ if its duration is $\Delta t << \tau_w$:

$$F_z^{iw} = C_{iw}(e^{-T} - e^{-\eta T}). \tag{27}$$

Here C_{iw} is C_w with J_w^0 replaced by J_0. This corresponds to $\alpha = 1$ in (24) to make $F_z^{iw}(0) = 0$, which is a general requirement for rapid events [7, 12]. It is clear that Eq. (27) gives F_z^{iw} identically zero afterwards, at $T > 0$, if $\eta = 1$. However, with $\eta > 1$, or $\tau_0 > \tau_1$ predicted by (21) and (22) and confirmed in [8, 16], we get instead a force F_z^{iw} developing as shown by the solid (blue) curve in Fig. 1.

Ultimately, the importance of this departure of $f_w(T)$ from zero depends on the amplitude coefficient C_{iw}. The numerical results in [7–10] and estimates reveal that C_{iw} can be large enough for producing a sizable F_z^{iw} at $T > 0$. This justifies the necessity of taking realistic $\eta > 1$ in the analysis. Let us recall that indication "ideal wall" (*iw*) refers only to the period of jump-like disruption. After that the wall is treated as a resistive shell with current evolution characterized by two time scales through T and η in (24) and (27). A difference between the cases with artificial $\eta = 1$ and realistic $\eta > 1$ can be impressive at $\alpha \neq 1$ too, especially at $\alpha > 1$.

6. THE ROLE OF α

Equations (23) and (24) show that, at given C_w, the initial post-disruption force is determined by $1 - \alpha$. The subsequent evolution of f_w is also affected by α. In the two-parametric family $f_w(\alpha, \eta)$, the areas with $\alpha > 1$

and $\alpha<1$ are naturally divided by the ideal-wall asymptote with $\alpha=1$ that provides F_z^{iw} given by (27). This must be strictly zero at $\eta=1$, which is a consequence of oversimplified (18). However, with $\eta>1$, the bracket in (27), vanishing at $t=0$ and $t\to\infty$, is positive in-between. The maximal deviation $\max(F_z^{iw}/C_{iw})=(1-\tau_1/\tau_0)\exp(-T_m^{iw})\equiv f_{\max}^{iw}$ occurs at $T_m^{iw}=(\eta-1)^{-1}\ln\eta$.

Equation (24) reveals two characteristic (normalized) times: $T_0\equiv(\eta-1)^{-1}\ln\alpha$, which is the moment when f_w passes through zero, and $T_m\equiv T_m^{iw}+T_0$, when $df_w/dT=0$. Note that, at $\alpha>0$, T_0 increases with α and crosses the point $T_0=0$ at the ideal-wall value $\alpha=1$. The behaviour of function $f_w(T)$ defined by (24) is shown in Fig. 1 for a tokamak with $\tau_0/\tau_1=2.6$ obtained from (21) and (22) at $R_w/b_w=3.4$. With this choice, we get $T_m^{iw}=0.6$ and $\max F_z^{iw}=0.34C_{iw}$. The uppermost curve corresponds to $\alpha=1/\eta=1/2.6$ with $T_m=0$ and $df_w/dT<0$ at $T>0$. The nearest one (the second from the top) with only small increase in f_w at $T>0$ is obtained for $\alpha=0.7$. The solid (blue) curve represents the "ideal-wall" scenario with $\alpha=1$ and non-zero force developing from $F_0=0$, and the lowest one gives us f_w at $\alpha=1.3$ (and $T_0=0.16$).

With $\alpha>1$, we have $f_w(0)=1-\alpha<0$, which is always accompanied by $f_w>0$ at $T>T_0>0$. The min-max span in f_w is $\alpha-1+f_{\max}$. In the particular case with $\alpha=1.3$, the curve in Fig. 1 starts from -0.3 and reaches a positive maximum slightly above 0.287 or $\approx 96\%$ of the initial amplitude. Such a half-oscillating behaviour of the force can be dangerous in excitation of a resonant response of the vessel. It was reported recently [5] that the whole vessel of the ASDEX Upgrade with its internal components oscillates after the disruption for almost one second. The force represented by the lowest curve in Fig. 1 can be a good reason for that.

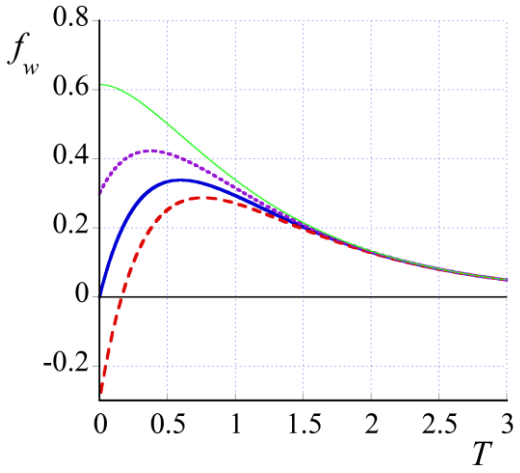

Fig. 1. Function $f_w=e^{-T}-\alpha e^{-2.6T}$ describing the time behavior of the post-disruption vertical force F_z^w. Here $T\equiv t/\tau_0$ and $\eta\equiv\tau_0/\tau_1=2.6$. The latter corresponds to $R_w/b_w=3.4$. From top to bottom: $\alpha=1/2.6$ (thin green curve), 0.7 (dotted violet), 1 (thick blue), and 1.3 (short-dashed red).

7. DISCUSSION

Fig. 1 demonstrates that a significant growth of the wall force is possible after the end of disruption. The curves in Fig. 1 look very similar to those presenting F_z^w in Figure 3 in [7], Figure 8 in [8], Figure 9 in [9], and Figures 4, 5 and 7 in [10], where the post-disruption force has been numerically calculated. See also the left plot in Figure 8 in [11] and Figure 11 in [5] with experimental data from the ASDEX-Upgrade tokamak. For certainty, in one example of the CarMa0NL computations, the post-CQ vertical force on the ITER wall exceeded 10 MN (Fig. 3 in [7], the curve crossing zero like the lowest curve in our Fig. 1). This should be taken into account in evaluation of the statement [17] that the vertical force on the vessel will be relatively small (less than 1 MN) if the CQ time of the disrupting plasma is shorter than the wall time constant.

Those particular results are covered by universal equation (23), where two general properties are accounted for. First, in the ideal-wall limit, the integral force on the VV wall cannot develop despite a high amplitude of the current induced in the wall [12]. In reality this means a low force during the events with duration much shorter than τ_w. Second, redistribution of the wall current occurs faster than the decay of its "slowest" harmonic described by $\exp(-T)$ in (24). This function is a common asymptote for all curves in Fig. 1 at $T>T_m$. These look indistinguishable at $T>1.5$. The pronounced differences in f_w at $T<1$ are related to the interplay of $J_w z_q$ and $J_s^w b_w$, see (17) and (24).

It is clear that the post-disruption force in tokamaks must depend only on the wall properties and initial distribution of the toroidal component of $\mathbf{j}$ in the wall. Without drivers, it can be represented as a sum of the

current modes $j_m(u)e^{-t/\tau_m}$ with u denoting the poloidal angle. Their decay times τ_m must decrease with their numbers m as approximately $1/m$. This allows to retain only a few lowest harmonics for evaluation of F_z^w. The sufficiency of three-mode response for description of the metallic structures in the task of plasma stability in ITER was earlier discovered in [16].

The replacement of this sum by Eq. (18) proposed in [4] is an unjustified simplification. First, it is simply incompatible with (19). Second, with inevitable [12] $F_z^w(0)=0$ after a rapid event, it leads to $\partial F_z^w/\partial t=0$ in drastic contradiction to numerical results in [7–10] and experimental experience. As illustrated by (23), at least two differently evolving modes are needed for compatibility of seemingly contradictive $F_z^w(0)=0$ in the ideal-wall limit [12] and $F_z^w\neq 0$ at $T>0$. Then we have to operate with two free parameters, the ratios j_0^w/j_s^w at $T=0$ and τ_0/τ_1 (or α and η in our compact notation).

With or without halo current, the vertical force on the wall is fully determined by interaction of the toroidal current in the system plasma + wall with poloidal field external to this system, see Eq. (1). Its consequence (17) reveals the key parameters. First of all, these are three integral currents: J, J_w and J_s^w. These can be measured with a simple set of internal and external coils. The knowledge of the halo currents is not needed.

The account for different decay times of j_ζ^w harmonics is vitally important for correct evaluation of F_z^w. The disregard of this invalidates the model proposed in [4] irrespective of its other (maybe, partially repairable) drawbacks revealed in [5]. The idea that just a few current modes must be sufficient for the VDE description was advanced in [16] based on numerical calculations. Here we confirm it by analytical relations that are ready for both numerical and experimental use.

REFERENCES

[1] TESTONI, P., *et al*, Status of the EU domestic agency electromagnetic analyses of ITER vacuum vessel and blanket modules, Fusion Eng. Des. **88** (2013) 1934.
[2] CLAUSER, C.F., JARDIN, S.C. FERRARO, N.M., Vertical forces during vertical displacement events in an ITER plasma and the role of halo currents, Nucl. Fusion **59** (2019) 126037.
[3] SCHWARZ, N. *et al*, The mechanism of the global vertical force reduction in disruptions mitigated by massive material injection, Nucl. Fusion **63** (2023) 126016.
[4] MIYAMOTO, S., A linear response model of the vertical electromagnetic force on a vessel applicable to ITER and future tokamaks, Plasma Phys. Control. Fusion **53** (2011) 082001.
[5] PAUTASSO, G., FABLE, E., and the ASDEX Upgrade Team, Reduced models for the maximum vertical force in a tokamak device, Nucl. Fusion **65** (2025) 056004.
[6] Progress in the ITER Physics Basis, Chapter 3, Nucl. Fusion **47** (2007) S128.
[7] PUSTOVITOV, V.D., RUBINACCI, G., VILLONE, F., On the computation of the disruption forces in tokamaks, Nucl. Fusion **57** (2017) 126038.
[8] YANOVSKIY, V.V., *et al*, Global forces on the COMPASS-U wall during plasma disruptions, Nucl. Fusion **61** (2021) 096016.
[9] ARTOLA, F.J., *et al*, Non-axisymmetric MHD simulations of the current quench phase of ITER mitigated disruptions, Nucl. Fusion **62** (2022) 056023.
[10] YANOVSKIY, V., *et al*, Sideways forces on asymmetric tokamak walls during plasma disruptions, Nucl. Fusion **62** (2022) 086001.
[11] SCHWARZ, N., *et al*, Experiments and non-linear MHD simulations of hot vertical displacement events in ASDEX-Upgrade, Plasma Phys. Control. Fusion **65** (2023) 054003.
[12] PUSTOVITOV, V.D., General approach to the problem of disruption forces in tokamaks, Nucl. Fusion **55** (2015) 113032.
[13] PUSTOVITOV, V.D., CHUKASHEV, N.V., Analytical solution to external equilibrium problem for plasma with elliptic cross section in a tokamak, Plasma Phys. Rep. **47**, 956 (2021).
[14] VANNINI, F., *et al*, Runaway electron beam formation, vertical motion, termination and wall loads in EU-DEMO, Nucl. Fusion **65** (2025) 046006.
[15] PUSTOVITOV, V.D., Extension of Shafranov's equilibrium theory to the description of current quenches affected by resistive wall dissipation in tokamaks, Plasma Phys. Rep. **45** (2019) 1114.
[16] PORTONE, A., The stability margin of elongated plasmas, Nucl. Fusion **45** (2005) 926.
[17] BANDYOPADHYAY, I., *et al*, MHD, disruptions and control physics: Chapter 4 of the special issue: on the path to tokamak burning plasma operation, Nucl. Fusion **65** (2025) 103001.